

Textile Composite Materials: Polymer Matrix Composites

Stepan V. Lomov and Ignaas Verpoest

Department MTM, Katholieke Universiteit, Leuven, Belgium

1 Introduction: What are Textile Composites?	1
2 Types of Textile Preforms	1
3 Behavior of Textile Preforms During Composite Manufacturing	6
4 Internal Structure of Textile Composites	6
5 Stiffness of Textile-Reinforced Composite	10
6 Strength and Damage Development in Textile-Reinforced Composites	11
7 Modeling Tools for Textile Composites	15
8 Conclusion	17
References	18
Further Reading	18

1 INTRODUCTION: WHAT ARE TEXTILE COMPOSITES?

Textile composites are fiber-reinforced composite materials, the reinforcement being in the form of a textile fabric (woven, knitted, braided . . .). In the *production* of composite parts, the use of textile reinforcements brings benefits in handability of the fabrics (hence in automation possibilities and in cost) and in easier applicability of closed-mold processes. In *performance*, due to interlacing of yarns in

textile, the interlaminar/through-the-thickness/impact properties of composite are improved; matrix cracks, originated inside the yarns, do not propagate through the material but are stopped when the yarn changes its direction. The latter mechanism leads to higher-energy absorption capabilities in crash-resistant applications.

The textile technology allows controlling of the placement of the yarns in the preform, opening ways to development of net-shape and 3D preforms. These benefits originate from the complex, well-organized internal structure of the fabric. The same internal structure, which is created by interlacing, hence waviness, of the yarns, leads to drawbacks in comparison with unidirectional laminates: lower stiffness of the composite due to inclination of fibers to the direction of the loading and somehow earlier damage initiation due to the presence of resin-rich zones created by the internal architecture of the textile.

Examples of applications are pressure bulkheads of A340 and A380 (non-crimp fabric (NCFs)); braided part of landing gear; 3D woven turbine blade. . . .

2 TYPES OF TEXTILE PREFORMS

“Textile” is defined as “. . . originally a woven fabric, but the term ‘textiles’ is now also applied to fibers, filaments and yarns, natural or man-made, and most products for which they are the principal raw materials” (*Textile Terms and Definitions*). Hence, textiles are *fibrous* materials. Fibers in a textile are assembled into yarns or fibrous plies, which are arranged to form a textile fabric.

2 Structural Materials

Textiles are *hierarchical* and *structured* materials with three levels of hierarchy: fibers (*micro*) – yarns/plies (*meso*) – fabrics (*macro*). The levels are characterized by

- Length scale (0.01 mm for fiber diameter, 0.1 mm yarns diameter, 1–10 mm for the dimensions of a representative element of a fabric);
- Dimensionality (fibers and yarns are one-dimensional objects, fabrics are two- or even three-dimensional);
- structural organization (fibers inside a yarn, yarns are woven to create a fabric).

The length scales inferior to the fiber diameter (internal structure of fibers and fiber/matrix interfaces) are not considered in this chapter, which focus on textile-structure-defined properties of composites.

On a given hierarchical level, one can think about a textile object as an entity and consider it, making abstraction of its internal structure: the yarn represented as a solid flexible rod (thread) or a woven fabric represented as a membrane. Properties of a textile are the properties of the fibers transformed by the textile structure, which is introduced deliberately during manufacturing.

Textile yarns, or *tows*, used in composite reinforcements, are characterized by the linear density of the yarns (measured in SI units $\text{tex} = \text{g km}^{-1}$) or fiber count in the yarns, the length of the fibers in the yarn (short or *staple* fibers, infinitely long *filaments*), the twist of the fibers measured in twists per m (flat yarns with straight fibers are called *rovings*). *Commingled* yarns can contain a blend of load-carrying fibers and thermoplastic resin in a form of short fibers or long filaments.

Textile reinforcements can be two-dimensional (2D) and three-dimensional (3D). A fabric is classified as 3D if there is a certain structural arrangement of the yarns in the thickness direction, and the integrity of the fabric is maintained with yarns which direction deviates significantly from the plane of the fabric. 3D fabrics normally have a considerable thickness, which is enough for the fabric to be used as a one-layer reinforcement. 2D fabrics, which have only in-plane arrangement of the yarns and are thin, are normally used in laminated preforms. A laminated preform can be stitched prior to the composite production; the stitched preform can be considered as an integral 3D reinforcement. 3D preforms and composites are described in 3D Translaminar and Textile Reinforcements for Composites.

2.1 Woven performs

A woven fabric is produced by interlacing of two orthogonal systems of yarns: warp (lengthway of the fabric) and weft or

fill (widthway). The repeating pattern of the interlacing, or *weave*, for a one-layered fabric is depicted by a checkerboard scheme (Figure 1). In such a scheme, each column of squares represents a warp yarn and each row – a weft yarn. A square is painted black if the warp yarn goes over the weft and white otherwise. Figure 1 shows the weaves most often used for composite reinforcements:

- *Plain weave*, with each warp yarn having an intersection with each weft yarn.
- *Twill*: a weave that produces diagonal lines on the face of the fabric. Depending of the *float* of the warp/weft yarns ($f_{\text{wa}}/f_{\text{we}}$, a number of subsequent crossings with correspondingly weft/warp on the same side of the fabric), a twill is designated as *twill* $f_{\text{wa}}/f_{\text{we}}$. The most used in composite reinforcements are twills 1/2, 1/3, and 2/2.
- *Satin*: a weave in which the binding places are arranged with a view to producing a smooth fabric surface. The crossings of warp and weft yarns are shifted at the neighboring yarns by a constant number of positions, which is called *step s*. The satin weaves are designated as N/s , where N is the repeat size. The most used in composite reinforcements are satins 5/1 and 8/1, also called five-harness (5H) and eight-harness (8H) satins (as they are produced on a loom with five and eight harnesses). A *crowfoot satin*, also often used in composites, is in the strict textile terminology, a *broken twill* 1/3 (twill with alternating direction of diagonal elements of the weave).
- *Basket*: a modified plain weave with two warp and two weft yarns running parallel.
- *2.5D weave*: this weave has two layers of weft and one layer of warp. The structure of such a fabric is easier to show using the trajectories of warp yarn, rather than the checkerboard pattern.

The weaves can be ranged according to the *tightness* of the weave (irrespective to the tightness of actual placement of the yarns) $T = N_{\text{links}}/(2N_{\text{tot}})$, where N_{links} is the number of transitions of warp or weft yarns from one side of the fabric to another and N_{tot} is the total number of the intersections ($=N^2$ for the case of square pattern). With the decrease of the tightness, (i) stability of the weave decreases, hence the fabric is easier to deform in draping of the preform, but also easier to be distorted in the process; (ii) average angle of inclination of the fibers to the middle plane of the fabric decreases, hence the average stiffness and strength of the composite increase.

Apart from the weave pattern, a woven fabric is characterized by linear density or fiber count in the yarns, ends/pick count (number of warps per unit width and number of wefts per unit length of the fabric), and areal density of the fabric. A *balanced* fabric has equal parameters in warp and

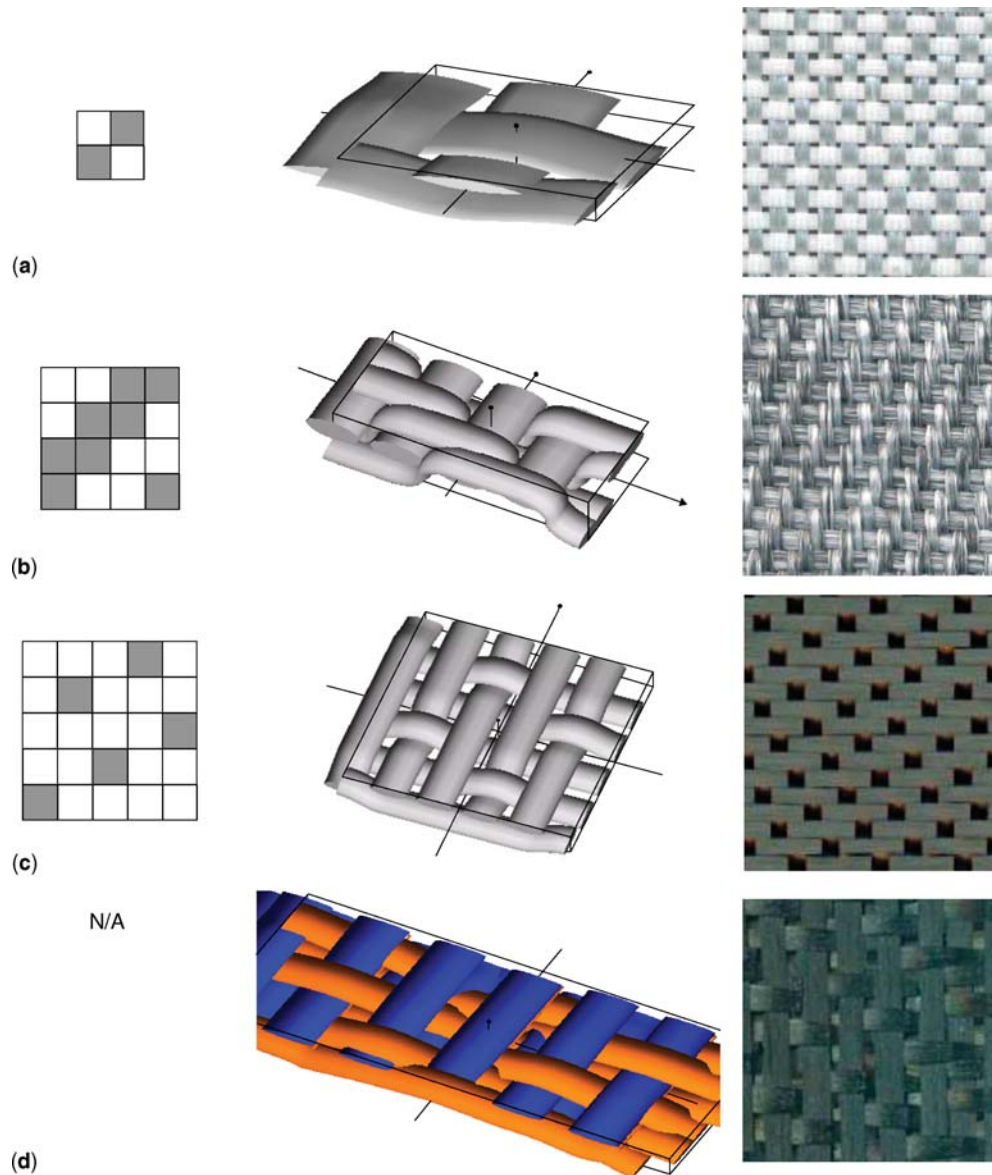


Figure 1. Weaves, 3D representations of the fabric repeat, and examples of composite reinforcements. (a) Plain weave, glass; (b) twill 2/2 weave, carbon; (c) 5H satin weave, carbon; (d) 2.5D weave, carbon.

weft directions; a *quasi-unidirectional* (UD) fabric has thick tightly placed warp yarns interlaced by thin sparse weft.

2.2 Braided performs

Braiding is the process of interlacing three or more threads in such a way that they cross one another in diagonal formation, as illustrated in Figure 2. Flat, tubular, or solid constructions may be formed in this way.

Patterns created by the braiding process are similar to the weaves and are designated using the same system as for twills, that is, a pattern is identified by length of floats of the

yarns of two interlacing systems. Three patterns have special names: *diamond* (1/1), *regular* or *plain* (2/2), and *Hercules* (3/3) braids. Note that the name “plain” is used differently for weaves and braids. The repeat of a braid is called *plait*, *stitch*, or *pick*. It equals the total number of yarns in a flat braid and to half of it in tubular braids.

The most important parameter of a braid is the braiding angle α (Figure 2c) – an angle between the yarns of two interlacing systems. If a 3D-shaped mandrel with a variable diameter is used then the take-up speed should be constantly adjusted to achieve a uniformity of the braiding angle. Varying the take-up speed one can also achieve a certain

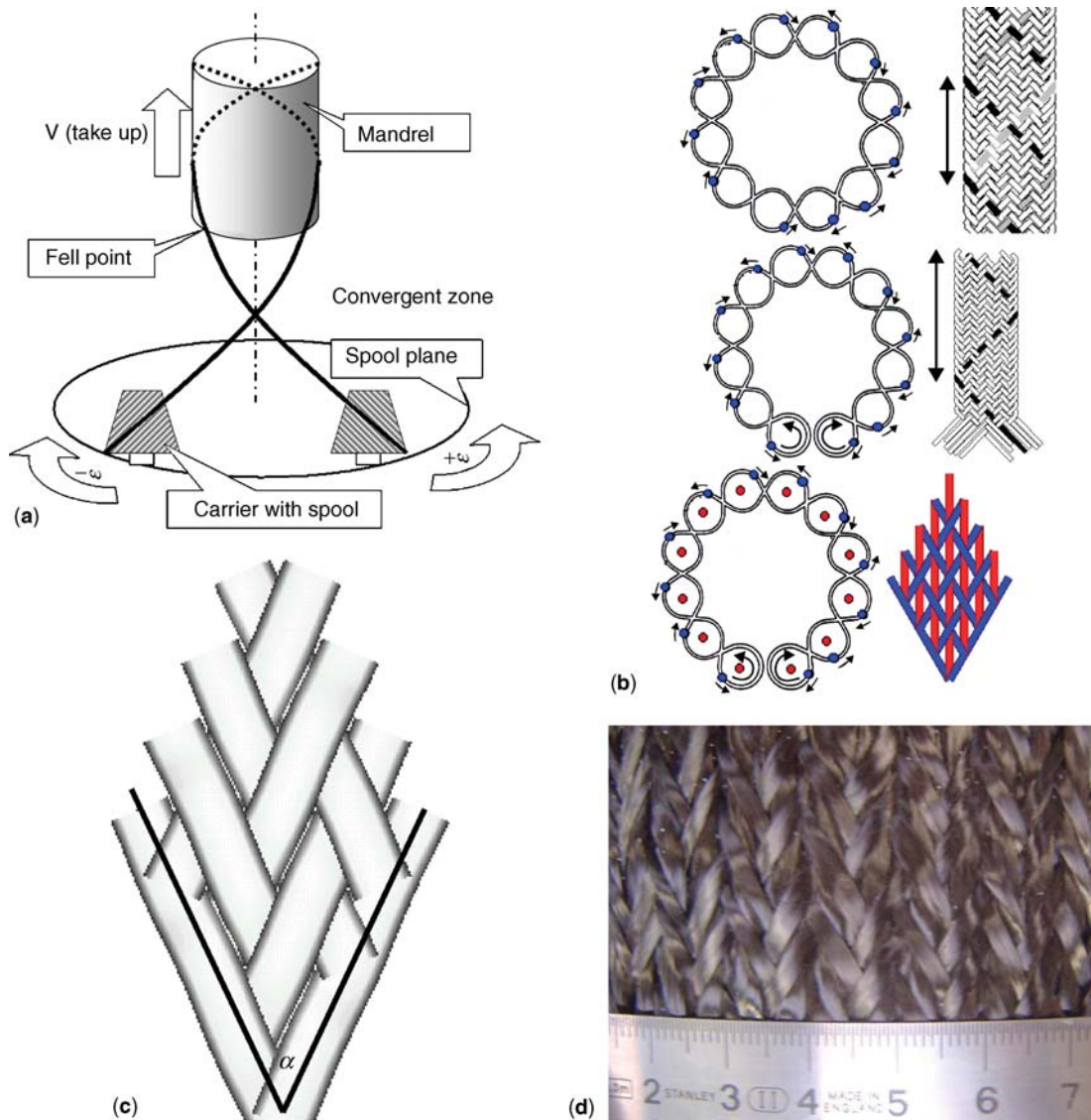


Figure 2. Braiding process. (a) Scheme of a maypole braider; (b) tubular and flat 2-axial braid and 3-axial braid: movement of the bobbins and interlacing scheme; (c) definition of the braiding angle; (d) carbon 3-axial braid $0^\circ/+60^\circ/-60^\circ$.

variability of braiding angles along the preform, resulting in a desired variation of stiffness of the composite part. The practical range of the braiding angle is between 20° and 160° .

When *axial* yarns are added to braiding yarns, then a three-axial braid is produced. In the particular case of a braiding angle of 120° , the three-axial braid produces a quasi-isotropic composite with fiber orientations $0^\circ/60^\circ/-60^\circ$.

2.3 Multiaxial multiply warp-knitted performs (non-crimp fabrics)

Non-crimp fabrics are designed to combine the unidirectionality of fibrous layers with the integrity of the preform, achieved by binding the layers together. European standard

EN 13473 defines a multiaxial multiply fabric as “A textile structure constructed out of one or more laid parallel non-crimped not-woven thread plies with the possibility of different orientations, different thread densities of the single thread plies and possible integration of fiber fleeces, films, foams or other materials, fixed by loop systems or by chemical binding systems. The threads can be oriented parallel or alternating crosswise. These products can be produced on machines with insertion devices (parallel-weft or cross-weft) and warp knitting machines or chemical binding systems”. A non-crimp fabric is characterized by the following parameters:

- fibrous nature of the plies (G – glass, C – carbon, A – aramid, etc.);

- areal density of the plies (g m^{-2}). It is not necessarily the same for all the plies;
- direction of fibers in the plies, given by an angle with the machine direction (0°). The angles lie in the range ($-90^\circ, -20^\circ$)($20^\circ, 90^\circ$);
- nature of the binding (PA – polyamide, PE – polyethylene, PES or PET – polyester, PP – polypropylene). This may refer to a stitching yarn or to a chemical binder;
- areal density of the binding;
- type of the binding agent (L – stitching or loop, C – chemical).

Binding the plies together by warp knitting can be deliberately made in such a way that the stitching yarn pierces the plies in between the laid threads. This would result in open preform architecture. Alternatively, wide threads (flat tows) are laid very close together, forming continuous fibrous plies. The plies are bound by warp knitting (Figure 3),

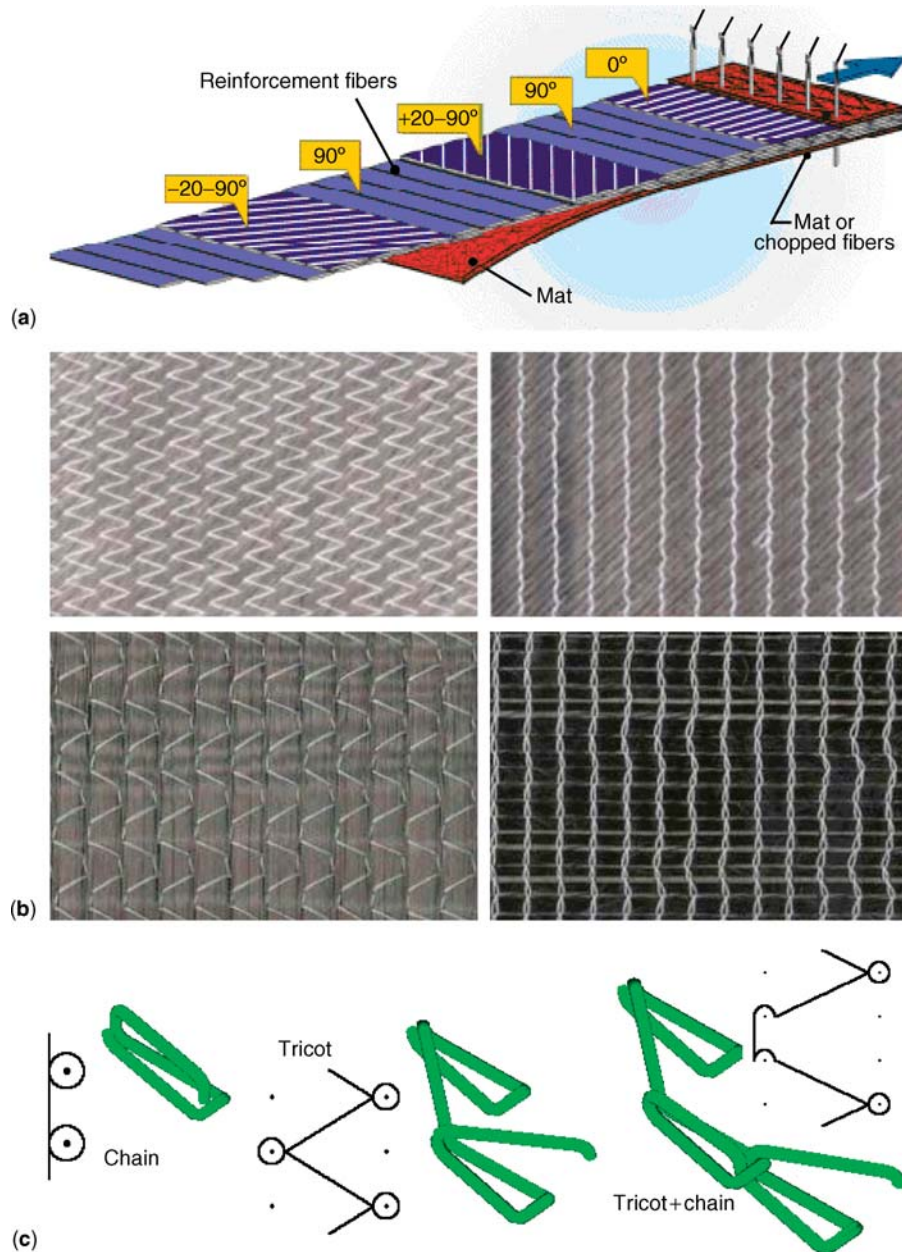


Figure 3. Non-crimp fabrics. (a) Scheme of the production process; (b) examples of NCFs: biaxial $+45/-45^\circ$ and $0/90^\circ$ fabrics, face and back sides; (c) typical knitting patterns used for NCFs.

with piercing sites positioned on the surface of the preform according to the needle spacing, without any connection to the tow positioning. Needles pierce the fibrous plies (probably in the middle of the laid-up tows), distorting them locally. This results in a preform construction close to an ideal laminate composed of unidirectional uniform plies.

3 BEHAVIOR OF TEXTILE PREFORMS DURING COMPOSITE MANUFACTURING

Composite manufacturing techniques, used for textile reinforcements, are covered in *Fiber-Reinforced Polymer Composites: Manufacturing and Certification Issues*. Two main processes involved during the manufacturing are shaping of a textile preform on a three-dimensional mold and impregnation of the preform with resin. The behavior of the preform during manufacturing is determined correspondingly by its *formability* and *permeability*.

3.1 Formability

The formability (drapability) of a textile fabric reflects the easiness of the initially flat fabric to conform to (drape over) a given 3D shape. The bending rigidity of textiles is very low (e.g., for a woven or NCF carbon reinforcement with areal density about 500 g m^{-2} , the bending rigidity per unit width of the fabric is about $0.1\text{--}0.2 \text{ N mm}^2 \text{ mm}^{-1}$ – compare with the bending rigidity of $730 \text{ N mm}^2 \text{ mm}^{-1}$ for an epoxy-impregnated plate made of one layer of such a fabric, with fiber volume fraction 60% and thickness 0.5 mm). Formability of the fabric is mainly determined by its resistance to in-plane shear deformations, and, to the lesser extent, by resistance to biaxial tension, through-the-thickness compressibility and friction (perform mold and between the preform layers).

The resistance of textile fabrics to shear deformation is measured using two types of tests: the picture frame test and (for biaxial woven, braided, and non-crimp fabrics) bias extension test (Figure 4). The load–displacement diagrams registered in these tests are processed to yield a *shear diagram*, showing the dependency of the shear force (normalized per unit width of the fabric sample) on the shear angle of the fabric. The *locking angle* is the value of the shear angle, which marks a fast increase of the shear deformation, caused by jamming of the yarns, coming too close during shearing and hence resisting further lateral compression. When shear reaches the locking angle at a certain place of the preform

during forming, this signals onset of wrinkling and hence unacceptable forming regime. The shear diagram is used as input to the forming modeling software as is, in its full non-linear form, or as a linear approximation of the first part of the diagram, bounded by the locking angle (Figure 4c).

3.2 Permeability

The permeability of the preform is a tensor coefficient \mathbf{K} of *Darcy equation*, relating the flow velocity of a fluid through the porous medium to the pressure gradient:

$$\langle \mathbf{u} \rangle = \frac{\mathbf{K}}{\mu} \nabla p \quad (1)$$

where $\langle \mathbf{u} \rangle$ is average velocity of the fluid flowing through the porous medium, μ is viscosity of the fluid, and ∇p is pressure gradient, causing the flow. The unit of \mathbf{K} is m^2 . The permeability is a geometrical characteristic of the porous structure of the medium (textile preform), which characterizes the easiness of the liquid (resin) to flow through the medium (to impregnate the preform). It strongly depends on the fiber volume fraction of the preform and on the internal geometry of the textile (Figure 5). Permeability is determined by either measuring the velocity of propagation of the flow front during impregnation of the preform (*unsaturated flow*) or by measuring the amount of fluid flowing through the preform (*saturated flow*) under given pressure difference. For denser reinforcements (or for denser regions inside a preform), wetting properties and capillary effects may play a role in the resistance to the flow. This is reflected in the differences of permeability measured by the saturated and the unsaturated flow method.

4 INTERNAL STRUCTURE OF TEXTILE COMPOSITES

As fibers and yarns in textiles are held together by friction, the yarns have to be bent or twisted to provide transversal forces, necessary for friction. The internal structure of a textile is the result of such bending of the yarns, introduced during manufacturing of the fabric. The internal structure determines the interaction between the fibers and yarns in dry fabric during manufacturing, transferring the applied load to structural fibrous elements of the fabric, which resist the load by their deformation (primarily tension, bending/buckling, lateral compression and friction, and to a lesser extent torsion and shear). The internal structure determines the performance of a consolidated composite as well: the stress response to the

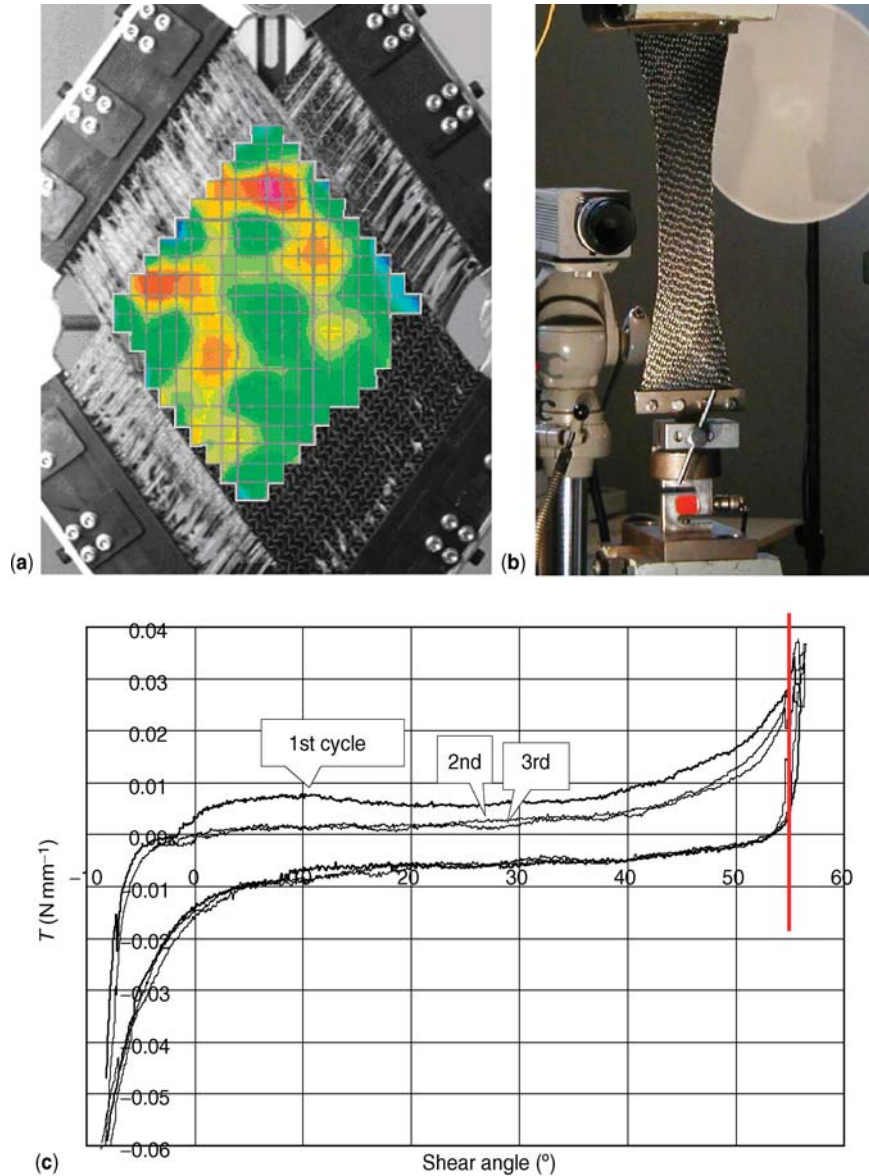


Figure 4. Deformability of textile fabrics. (a) Picture frame tests; (b) bias extension test; (c) typical shear diagram (NCF), definition of the fabric-locking angle.

local deformation depends on the local orientation of fibers, which is imposed by the reinforcement architecture, and in its turn defines whether damage will be initiated in that particular location and whether it will propagate.

The internal structure of textiles is periodic. The smallest element of periodicity is called the *unit cell* or *repeat* of the structure (see examples of woven unit cells in Section 2 above). The shape of the yarn inside a unit cell can be defined by the yarn path and by the dimensions and orientations of the yarn cross section along the path (Figure 6a and b). The dimensions of the yarn cross section can vary along the path

due to the interaction between the yarns. The shape of the yarn is defined by these interactions and can be calculated based on principle of minimum energy of deformation of the yarn (bending + lateral compression). When the end positions of the *bent intervals* of the yarns (“anchor points” of the yarn path) are known (points A and B, Figure 6c), the shape of the yarn in the interval can be described (i) by an elastic line between these end points or (ii) by a contact with the supporting contours of the intersecting yarns. Both approaches are approximate and can be refined by finite element modeling of the yarn interaction.

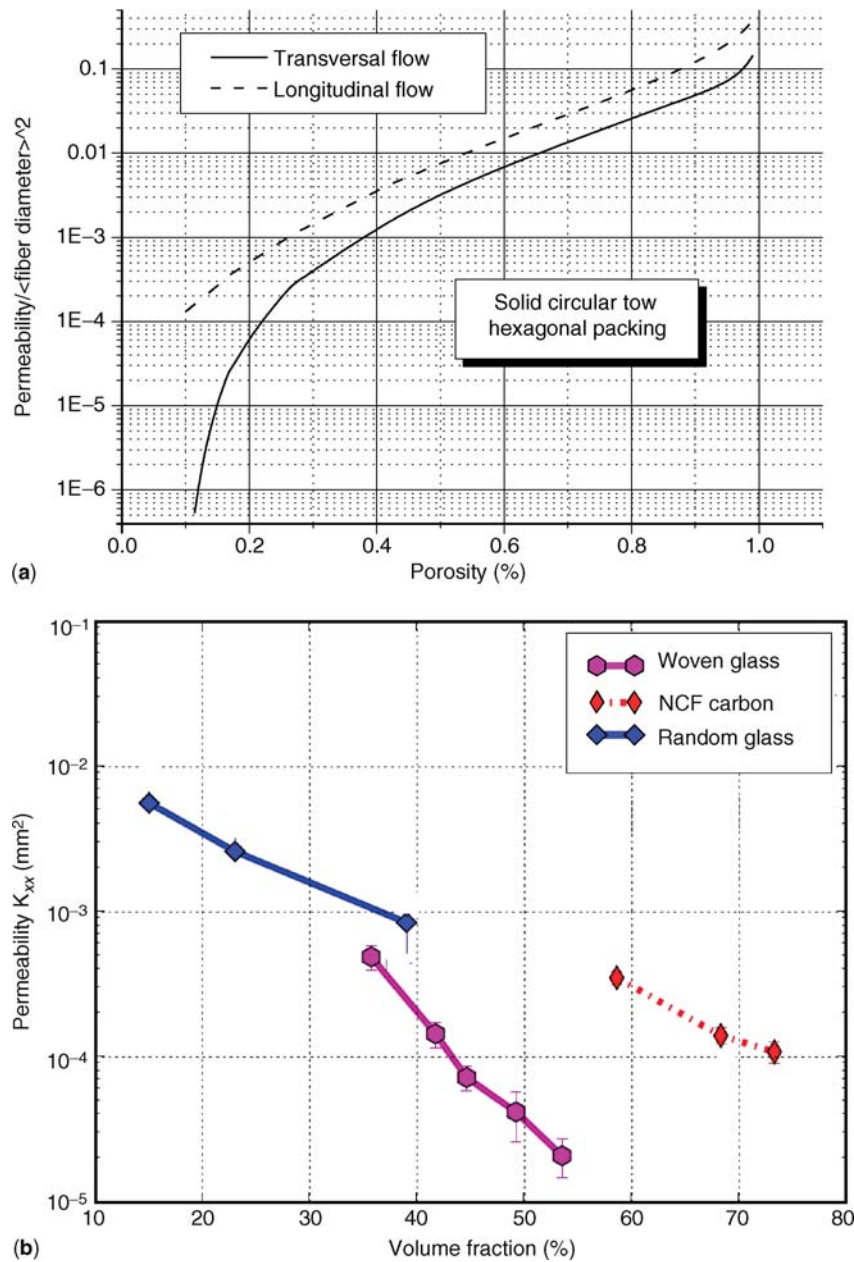


Figure 5. Permeability as function of fiber volume fraction for (a) unidirectional array of fibers, longitudinal and transversal flow; (b) different textile preforms.

4.1 Crimp

The waviness of a yarn is measured by its *crimp*

$$c = \frac{l - l_0}{l} \tag{2}$$

where l is the length of the yarn in the unit cell, l_0 is the straight distance between end points of the yarn. Crimp is

connected to the inclination of the yarn, which defines the reduction of stiffness of the composite. For a balanced plain weave, the fabric crimp and the maximum inclination angle θ_{max} can be calculated by approximate formulae

$$c = \frac{bN}{80}(1 + 10bN); \quad \theta_{max} = \arctan \frac{bN}{6} \tag{3}$$

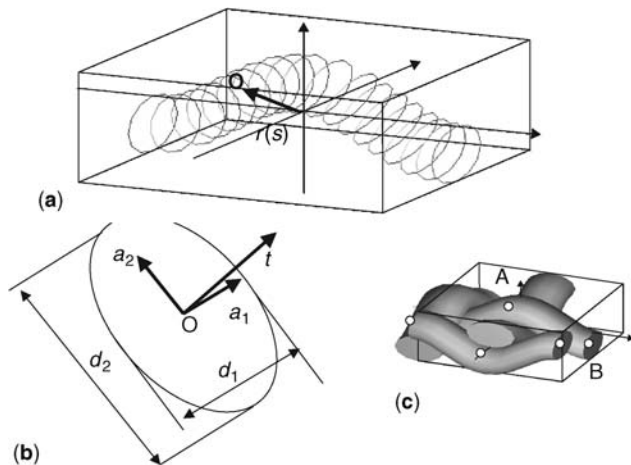


Figure 6. Yarns in textile unit cell. (a) General description of the yarn volume; (b) definition of the cross section; (c) bent element of the yarns.

where b is the fabric thickness (double the yarn thickness), N is yarn count per unit length/width of the fabric. For typical values (glass fabric with areal density of about 800 g m^{-2}) of $b \cong 0.6 \text{ mm}$, $N \cong 21 \text{ cm}^{-1}$, these formulae give $c = 0.3\%$, $\theta_{\max} = 1.1^\circ$.

4.2 Pores, resin-rich zones, nesting

Apart from the yarn crimp, another distinctive feature of the textile preform are the pores between yarns. The pores, on one

hand, facilitate impregnation of the preform, creating channels for resin flow. On the other hand, pores create resin-rich zones in the composite, leading to stress/strain concentrations and possibly earlier onset of damage in comparison with UD cross-ply laminates.

The surface of a textile fabric is not flat; it exhibits “hills” and “valleys”. When a laminated preform is being compacted in composite manufacturing, the layers of the laminate are not precisely positioned one against another, causing a geometric and mechanical phenomenon of *nesting*, when the “hills” and “valleys” of the contacting layers match one with another. This causes a smaller laminate thickness and a higher volume fraction of the laminate. Nesting plays an important role in determining the permeability of the laminate and the mechanical properties of the composite. It causes a statistical distribution of the laminate properties, both at different positions within a composite sample and between different samples in a set of otherwise identical parts. Nesting can be characterized by a *nesting coefficient* – reduction of thickness of a laminate in comparison with the thickness of the one-layer plate produced under the same pressure.

The nesting of a typical woven laminate (Figure 7a) is characterized by a nesting coefficient of about 0.9. Note that the “gaps” between certain layers, which have matching “hills” of the neighboring surfaces, may lie close in one and far in another position in the plate due to statistical scatter of distance between the yarns. Due to non-orthogonal interlacing, which causes certain twist of the flat rovings, braided fabrics exhibit profound nesting, with a nesting coefficient

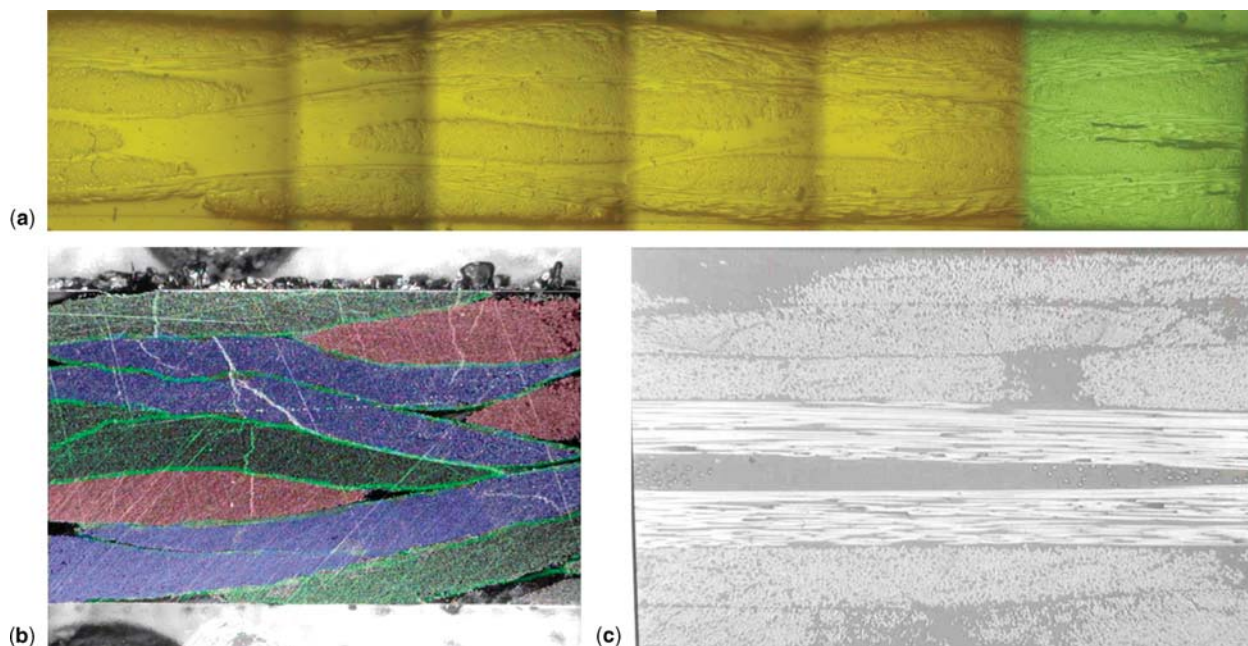


Figure 7. Internal structure and nesting. (a) Woven laminate; (b) braid; and (c) NCF.

reaching 0.6 (Figure 7b). NCFs have a system of pores/resin-rich zones in a form of *openings* and *channels*; due to presence of the stitching yarn on the face of the fabric, a thin gap can be formed between the layers of laminated NCF (Figure 7c).

5 STIFFNESS OF TEXTILE-REINFORCED COMPOSITE

Due to the inherent symmetry of as-produced textile fabrics, textile composite plates are orthotropic for the most types of the reinforcement (woven, braided, practically used layouts of NCF). Their stiffness can be represented by engineering constants: Young modules E_{ii} , shear modules G_{ij} , and Poisson coefficients ν_{ij} , $i, j = 1, 2, 3$. For non-orthogonal reinforcements (braids, sheared woven fabrics), the directions of orthotropy do not coincide with fiber directions. If the reinforcement is deformed during production of the composite, or if the preform is net shaped, or for some knitted performs, then the assumption of orthotropy does not necessarily apply and the full stiffness matrix has to be introduced.

The stiffness of textile reinforcements made of yarns, which are straight in plane, can be calculated as a first rough approximation, using the Classical Laminate Theory (CLT), which considers an equivalent cross-ply laminate with ply directions corresponding to the principal directions of the yarns in the textile composite, the thickness and fiber volume fraction is the same as in the textile composite and the thickness of the plies is proportional to the amount of the fibers with the corresponding direction. Such a calculation provides overestimation of the textile composite stiffness because yarn crimp causes deviation of the fiber directions from the cross-ply laminate model. For the engineering constants in fiber directions, the CLT-calculated modules can be corrected using empirical *knock-down* factors, which would account for crimp. With low out-of-plane inclination angles, such a calculation gives acceptable results, especially for modules in the fiber direction.

For textile composites where the yarns are crimped (in-plane crimp, as in knits, or out-of-plane, as in woven fabrics or braids, or more complex 3D crimp), more elaborate approaches have to be used. Calculation of the homogenized stiffness must take into account the fact that the fibers are organized into impregnated yarns, hence the homogenization calculation should be in two steps: first, homogenize the stiffness of the impregnated yarns, and, second, homogenize the stiffness of the unit cell, taking into account their orientation.

Impregnated yarns are considered as UD-reinforced composites (twist of the yarns used in composite reinforcement is normally negligible) with the given fiber volume fraction

V_f^y ; this value is determined by the dimensions of the cross section of the yarn (which can differ from point to point in the unit cell but most often assumed to be constant) and the amount of fibers inside the yarn, given by the fiber count or yarn linear density:

$$V_f^y = \frac{T_y}{A_y \cdot \rho_f} = \frac{N_f A_f}{A_y} \quad (4)$$

where T is linear density of the yarn, A – cross-section area of the yarn, ρ – density of the fibers, N_f – number of fibers in the yarn, subscript “f” means “fiber”, “y” – “yarn”. With the fiber volume fraction V_f^y given, homogenized stiffness of the impregnated yarn can be calculated using one or another set of micromechanical formulae for UD plies, for example, Chamis formulae (Chamis, 1989):

$$\begin{aligned} E_{11}^y &= V_f^y E_{11}^f + (1 - V_f^y) E_m \\ E_{22}^y &= E_{33}^y = \frac{E_m}{1 - \sqrt{V_f^y} \left(1 - \frac{E_m}{E_{22}^f}\right)} \end{aligned} \quad (5)$$

$$\begin{aligned} G_{12}^y &= G_{13}^y = \frac{G_m}{1 - \sqrt{V_f^y} \left(1 - \frac{G_m}{G_{12}^f}\right)} \\ G_{23}^y &= \frac{G_m}{1 - \sqrt{V_f^y} \left(1 - \frac{G_m}{G_{23}^f}\right)} \end{aligned} \quad (6)$$

$$\nu_{12}^y = \nu_{13}^y = V_f^y \nu_{12}^f + (1 - V_f^y) \nu_m \quad \nu_{23}^y = \frac{E_{22}^y}{2G_{23}^y} - 1 \quad (7)$$

where E is the Young modulus, G – shear modulus, ν – Poisson coefficient; sub- or superscript “f” means “fiber”, “y” – “yarn”, “m” – matrix; axis 1 of the Cartesian co-ordinate system 123 is aligned with the fiber direction.

Once the homogenization of the impregnated yarns is performed, the homogenized stiffness of the textile composite can be calculated using different methods (see Section 6). The simplest one, *orientation averaging* (also called *fabric geometry model*), uses the iso-strain assumption for the unit cell of the textile composite and calculates the homogenized stiffness of the composite as

$$\begin{aligned} \mathbf{C}^{\text{eff}} [\text{GCS}] &= \mathbf{C}^m [\text{GCS}] \cdot (1 - V_y) \\ &+ \sum_{i=1}^N \mathbf{C}_i^y [\text{CS}_i \rightarrow \text{GCS}] \cdot V_y^i; \quad V_y = \sum_{i=1}^N V_y^i \end{aligned} \quad (8)$$

where C^{eff} is averaged stiffness matrix of the composite, C^{m} – stiffness of the matrix, C^{y} – homogenized stiffness of the impregnated yarns; V_{y} is the total volume fraction of the impregnated yarns. All the stiffness matrices are written in the global coordinate system (GCS). Based on the geometry of the reinforcements, N groups of segments of the yarns are defined inside the unit cell, so that inside a group i , the orientation of the fibers (or center line of the yarn) is approximated by the coordinate system CS_i , aligned with the fibers. V_{y}^i is the volume fraction of the impregnated yarn segments belonging to the group i .

Table 1 gives typical values of stiffness of different textile composites, calculated using the orientation averaging formulae, in comparison with properties of UD material and cross-ply laminates. Note intuitively non-evident effects appearing even for a simple plain weave composite: while for carbon (low-transverse fiber properties, hence low transverse and shear stiffness of the impregnated yarns), the moduli in the fiber direction are higher for cross-ply laminate than for woven composite, and for glass (isotropic fibers, hence higher transverse and shear properties of the impregnated yarns) the relation is inverse (this effect is also observed experimentally).

The high stiffness of composites requires a precise measurement of deformations during testing. Optical extensometry – full-field strain measurement methods (e.g., digital image correlation, interferometry, grating shearography) – allow not only precise measurement of average displacements and hence strains over the sample, but also provide a strain field over the surface, correlated with the geometry of the textile reinforcement. Analysis of the strain field reveals locations of strain maxima, correlated with the sites of the damage onset (Figure 8).

6 STRENGTH AND DAMAGE DEVELOPMENT IN TEXTILE-REINFORCED COMPOSITES

6.1 Quasi-static tensile strength and damage

Textile composites fail under tensile loading as a result of a long and complex series of damage events. These events happen on different hierarchical levels of the composite structure: fibers in the impregnated yarns (*micro*), yarns and matrix pockets in the unit cell of the textile reinforcement (*meso*), composite plies forming a plate or 3D part (*macro*). On each of these structural levels, stress–strain concentrations happen at heterogeneities of the material (boundaries between interlacing yarns with different directions and between the yarns and resin pockets, fiber/matrix interface).


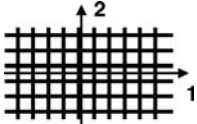
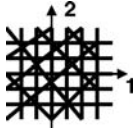
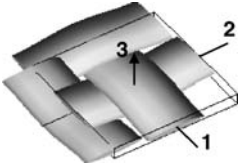
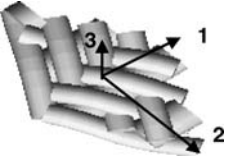
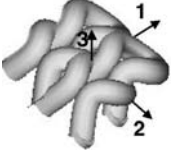
These damage events can be revealed in a test instrumented with an acoustic emission (AE) device and can be more closely observed in tests stopped at certain stages of loading. The damaged samples can be inspected by ultrasonic C-scan, under X-ray or (transparent samples) optically; they also can be cross sectioned and damage studied under microscope. Figure 9 illustrates such a test for a transparent glass/epoxy plain weave composite.

At the very beginning of the test, there are no acoustic events registered. Further, starting from certain load threshold, characterized by strain ε_{min} (*AE threshold strain*), low-energy acoustic events start to occur, though quite rarely. These events result from micro-cracking in the matrix and/or fiber debonding. Then, their occurrence rate and the energy associated with these events start increasing sharply, and soon the energy content reaches higher levels. Micro-cracks at fiber/matrix interface coalesce and form transverse and shear matrix cracks inside impregnated yarns. This is reflected by the increase of the slope of the cumulative AE energy curve, which was negligible before. The corresponding *first damage threshold strain* is designated ε_1 . This value is identified as the *damage initiation threshold*, as it corresponds to a substantial change of slope of the respective stress–strain curve. The damage accumulated between ε_{min} and ε_1 strain levels is not sufficient to deteriorate the tension resistance enough to affect the overall stiffness of the test sample. At some higher level of the applied strain, a second “knee” on the AE cumulative energy curve may appear, corresponding to the *second damage threshold strain* ε_2 . This corresponds to extensive damage on the scale spanning several unit cells of the reinforcement, for example, delaminations between woven plies.

As shown in Figure 9, when a woven composite is loaded in warp direction, the initial cracks are parallel to the weft direction. The length of these cracks roughly corresponds to that of the weft yarn segment contained between two adjacent crossovers of the warp and weft yarns. Due to the randomness of nesting of the layers of the plain weave fabric within the composite laminate, it is impossible to determine the exact location of these cracks using the transmitting light image. These cracks are transverse cracks within the weft yarns, as is confirmed by micrographs in Figure 9: typical pairs of the cracks at the distance roughly $\frac{1}{2}$ of the width of the yarn. As the load increases, the transverse cracks multiply and become longer, with the length sometimes spanning over several unit cells. A system of long, well-developed multiple cracks oriented perpendicular to the loading direction forms; they split the weft yarns and generate large delaminated regions between the layers of plain weave fabric. Additionally, a multitude of transverse cracks in matrix pockets is observed. Finally, fibers are broken and the sample fails.

12 Structural Materials

Table 1. Typical values of engineering stiffness parameters of UD, cross-ply and textile glass/epoxy, and carbon (HS)/epoxy composites.

Reinforcement	Image and coordinate system (for laminates: axis 3 is normal to the image plane)	Carbon/epoxy			Glass/epoxy		
		E_{11} (GPa) E_{22} E_{33}	G_{12} (GPa) G_{13} G_{23}	ν_{12} ν_{13} ν_{23}	E_{11} (GPa) E_{22} E_{33}	G_{12} (GPa) G_{13} G_{23}	ν_{12} ν_{13} ν_{23}
UD		139	4.0	0.25	44	4.0	0.25
		7.6	4.0	0.25	10	4.0	0.25
		7.6	2.5	0.37	10	3.5	0.37
Cross-ply 0/90		73	4.0	0.02	27	4.0	0.09
		73	3.2	0.35	27	3.7	0.34
		7.6	3.2	0.35	10.3	3.7	0.34
Quasi-isotropic 0/45/-45/90		52	20	0.31	21	8.2	0.29
		52	3.2	0.25	21	3.7	0.26
		7.6	3.2	0.25	10	3.7	0.26
Plain woven, crimp 0.5%		72	6.6	0.02	30	6.7	0.12
		72	5.4	0.39	30	6.4	0.31
		9.0	5.4	0.39	16	6.4	0.31
Tri-axial braid 0/60/-60, crimp braiding yarns 1%		61	24	0.32	30	12	0.27
		47	7.4	0.27	28	9.2	0.25
		9.9	6.3	0.25	23	9.0	0.26
Knitted jersey		27	14	0.22	24	10	0.25
		24	22	0.43	23	12	0.30
		27	14	0.18	24	10	0.24

Fiber volume fraction 60%.

Fiber and matrix data used in the calculations are as follows:

Carbon: $E_1 = 230$ GPa, $E_2 = 14$ GPa, $\nu_{12} = 0.23$, $\nu_{23} = 0.3$.

Glass: $E_1 = E_2 = 72$ GPa; $\nu_{12} = \nu_{23} = 0.23$.

Epoxy: $E = 3.0$ GPa, $\nu = 0.3$.

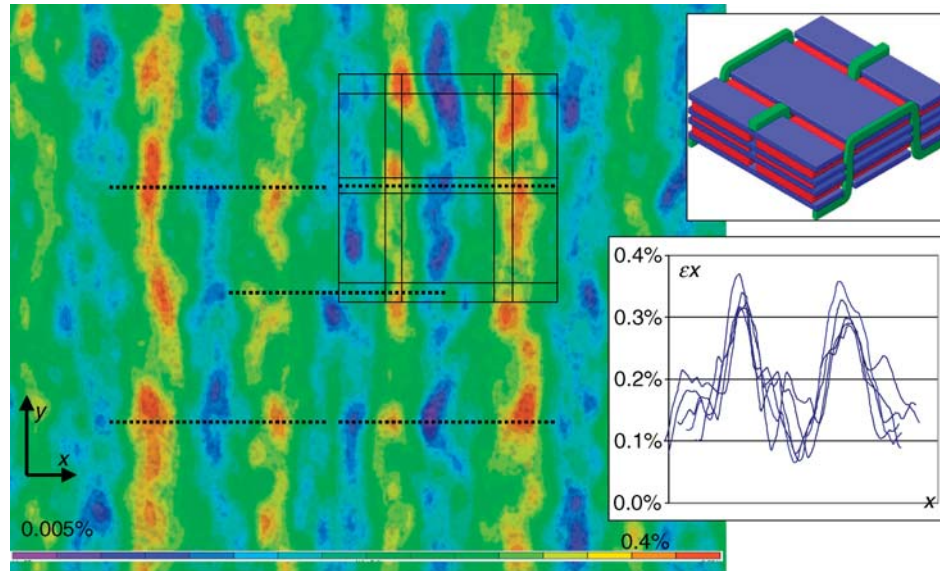


Figure 8. Full-field optical (digital image correlation) measurement of the surface strain in 3D woven composite. Surface strain maps for ε_x component before the damage initiation. Loading in horizontal (x) direction, average strain 0.2%. Inset top: the scheme in full lines shows location of the unit cell. Inset bottom: profiles of ε_x along the dashed lines, shown on the strain map.

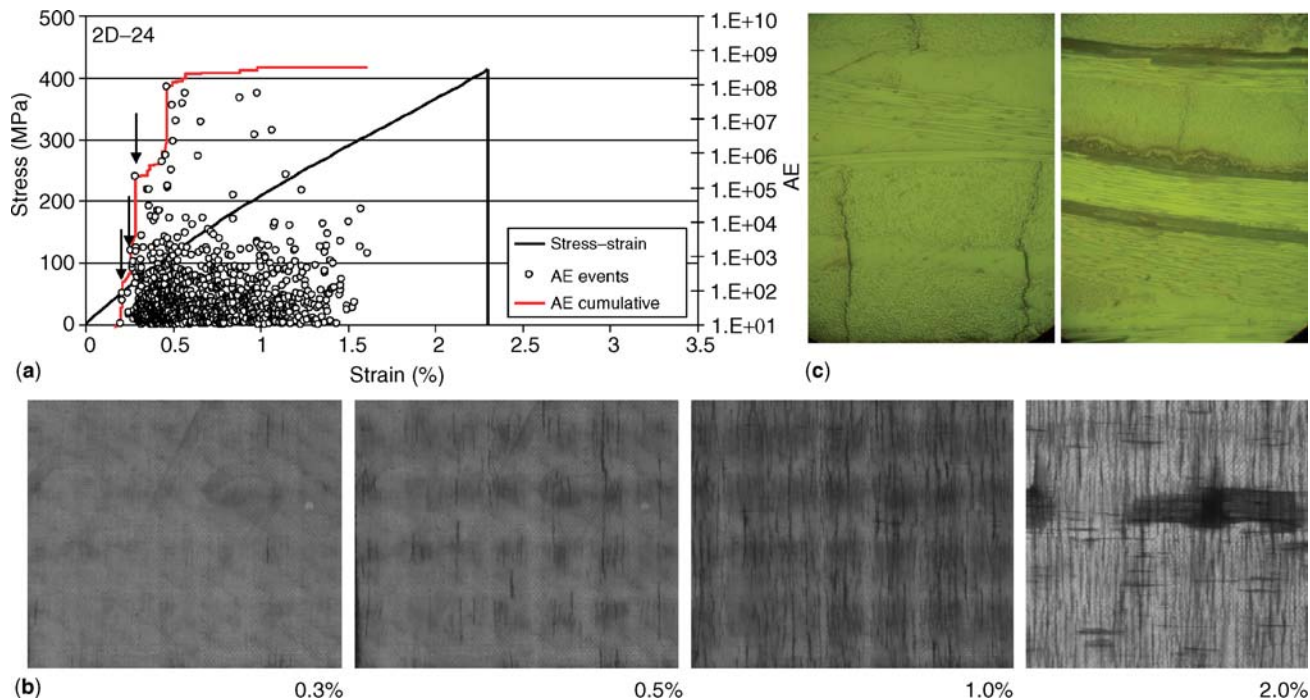


Figure 9. Damage initiation and development during tensile loading of plain weave glass/epoxy composite. (a) Stress–strain and AE diagram and damage thresholds; (b) damage evolution (transparent sample), loading in horizontal direction, applied strain is indicated; (c) damage at 2% strain and typical cracks: transversal and delaminations.

6.2 Compression and out-of-plane loading

The behavior of textile composite laminates (2D textile reinforcements) in compression, bending, and other types of

out-of-plane loading is controlled by the same phenomena as for UD laminates: delamination in different modes, fiber kinking, matrix shear failure – with the peculiarities in behavior defined by the architecture of the textile reinforcement.

The main factors affecting the damage behavior are the waviness (crimp) of the yarns and fibers and the nesting of the textile layers. These two geometrical features

- change the conditions of crack propagation of Mode I and Mode II delaminations, deviating the crack from a flat trajectory and increasing the apparent energy needed for crack propagation;
- in compression, facilitate the onset of fiber buckling, hence decreasing the compression strength;
- in crash, lead to multiple cracking increasing the effectiveness of energy consumption;
- in transverse impact, limit delamination area and increase energy absorption.

The qualitative characteristics of these changes of behavior in comparison with UD laminates depend very much on the concrete reinforcement type and details of its geometry. Experimental data can be found in the recommended literature.

6.3 Failure criteria for complex loading

For textile composites, failure can be predicted using different criteria, one of which is Hashin criterion for woven fabrics, which is implemented in several finite element packages for structural analysis. It defines six failure indices F : four for fiber damage (superscript f): warp and weft directions (subscripts 1 and 2) and tension and compression (subscripts t and c)

$$\begin{aligned}
 F_{1t}^f &= \left(\frac{\sigma_1}{X_t}\right)^2 + \left(\frac{\sigma_{12}}{S_{12}}\right)^2 + \left(\frac{\sigma_{13}}{S_{13}}\right)^2, \sigma_1 > 0 \\
 F_{1c}^f &= \left(\frac{\sigma_1}{X_c}\right)^2 + \left(\frac{\sigma_{12}}{S_{12}}\right)^2 + \left(\frac{\sigma_{13}}{S_{13}}\right)^2, \sigma_1 < 0 \quad (9) \\
 F_{2t}^f &= \left(\frac{\sigma_2}{Y_t}\right)^2 + \left(\frac{\sigma_{12}}{S_{12}}\right)^2 + \left(\frac{\sigma_{23}}{S_{12}}\right)^2, \sigma_2 > 0 \\
 F_{2c}^f &= \left(\frac{\sigma_2}{Y_c}\right)^2 + \left(\frac{\sigma_{12}}{S_{12}}\right)^2 + \left(\frac{\sigma_{23}}{S_{23}}\right)^2, \sigma_2 < 0 \quad (10)
 \end{aligned}$$

and two for matrix failure (superscript m) – onset of cracking in the impregnated yarns under through-the-thickness and shear stresses:

$$\begin{aligned}
 F_t^m &= \left(\frac{\sigma_3}{Z_t}\right)^2 + \left(\frac{\sigma_{12}}{S_{12}}\right)^2 + \left(\frac{\sigma_{13}}{S_{13}}\right)^2 + \left(\frac{\sigma_{23}}{S_{12}}\right)^2, \sigma_3 > 0 \\
 F_c^m &= \left(\frac{\sigma_3}{Z_c}\right)^2 + \left(\frac{\sigma_{12}}{S_{12}}\right)^2 + \left(\frac{\sigma_{13}}{S_{13}}\right)^2 + \left(\frac{\sigma_{23}}{S_{12}}\right)^2, \sigma_3 < 0 \quad (11)
 \end{aligned}$$

where stresses $\sigma_{ij}, i = 1, 2, 3$, are average stresses in the woven composite, X_t, X_c, Y_t, Y_c are strength values for the composite in the warp (X) and weft (Y) directions, respectively, Z_t, Z_c are transversal UD strength values in tension and compression, and $S_{ij}, i = 1, 2, 3$, are shear strength values for the composite.

Note that Hashin (and the similar) criterion does not predict in full the onset of matrix transverse and shear cracking in the yarns, which run at 90° and bias direction to the loading. Because of the complexity of the damage processes, the simple concept of “first ply failure” and “last ply failure” has not much meaning for textile composites, apart, probably, for NCF, where it is possible to treat UD plies inside the fabric separately. Consider, for example, a woven composite and Hashin failure index for loading in fiber direction. When entered in the ply failure index, strength of the ply in both principal directions means fiber failure, that is, the end of the complex process described above. This is in contrast with the “first ply failure” of a cross-ply laminate, which is controlled by transverse strength of the ply. For woven fabrics, such a state would correspond to transverse cracking of the weft (warp loading); hence, the parameters of stress in the damage criterion should correspond to the ε_1 threshold, described above. However, such information is not readily available for textile composites and requires advanced experimental techniques.

The simplicity of the quadratic failure criterion reflects its phenomenological nature. More advanced, physically motivated criteria exist for UD cross-ply laminates; these criteria are discussed in detail in Hinton, Kaddour and Soden (2004). These criteria can be used also for NCF composites, which are essentially UD plies laminates with fiber distortions originated from the stitching. However, these criteria cannot be applied directly to woven and braided composites, where directions of the fibers vary significantly from point to point inside a ply. They are used locally as an element of meso-FE damage analysis, described in the Section 7.4.

The damage progression is covered by criteria, which introduce damage variables. The most developed model of this type applied for textile composite laminates is based on the works of Ladevèze. Damage is considered as a weakening of the material due to all kinds of mechanisms (matrix cracking, fiber-matrix debonding, fiber failure...), which occur prior to the final failure of the sample. The stiffness of the material is degraded with the damage progression (change of damage variables d). For example, for in-plane loading, the stress–strain relation for the damaged material is given by

$$\begin{bmatrix} \varepsilon_1 \\ \varepsilon_2 \\ \gamma_{12} \end{bmatrix} = \begin{bmatrix} 1/E_1(1-d_1) & -\nu_{12}/E_1 & 0 \\ -\nu_{21}/E_2 & 1/E_2(1-d_2) & 0 \\ 0 & 0 & 1/G_{12}(1-d_{12}) \end{bmatrix} \begin{bmatrix} \sigma_1 \\ \sigma_2 \\ \tau_{12} \end{bmatrix} \quad (12)$$

where the compliance matrix shows degradation of Young moduli E_1 , E_2 and shear modulus G_{12} with the damage parameters d_1 , d_2 , and d_{12} . The dependence of the damage parameters on the applied load should be identified with a set of well-defined experiments, which adapt the set of identification experiments for UD laminates (Ladevèze and Le Dantec, 1992) to the particular case of textile composite under consideration. For woven laminates, for example, these include tension and compression in warp and weft direction and quasi-static cyclic tests in 45° direction. In more elaborate versions of this approach, the damage parameters can depend on the damage mode. The approach of Ladevèze is implemented in PAM-CRASH software; the details of application to textile composites could be found in Greve and Pickett (2006).

7 MODELING TOOLS FOR TEXTILE COMPOSITES

Modeling of textile composites may be considered at different structural levels: *meso-level*, describing dependency of overall, homogenized properties of the material on its internal structure and on the properties of the constituents (fibers and matrix), and *macro-level*, describing either the manufacturing process (forming, impregnation. . .) or in-service (mechanical, thermal. . .) behavior of a composite part, based on the homogenized (but not necessarily constant) properties of the composite. Figure 10 illustrates the multi-level structure of models of textile composites. A *unit cell* approach is used: the properties of the textile reinforcement (resistance to deformation, permeability. . .) or textile composite (stiffness, strength. . .) are calculated for the unit cell, or representative (or repetitive) volume element (RVE) of the

reinforcement, which has translational symmetry inside the textile structure.

7.1 Geometrical model of the unit cell

The geometrical model of the unit cell is the core of the multi-scale modeling approach. It starts from the coding of textile architecture, using, for example, a weave matrix or a knitting scheme. The structure coding defines the interlacing pattern of the yarns. Using information on the density of the textile (ends/picks count for weaves, pitch for braids, gauge for knits), the modeling algorithms translate the interlacing pattern into a geometrical definition of the yarn paths in the unit cell space. This calculation may have user-defined input of crimp of the yarns or use a mechanical model of interlacing of yarns. In the latter case, the bending and compression resistance of the individual yarns should be provided. Finally, assigning shape and dimensions of the yarn cross sections (variable along the yarn path), the geometry of the unit cell is built.

Two major software packages exist for geometrical modeling of textile reinforcements: *TexGen* (<http://texgen.sourceforge.net>) and *WiseTex* (Verpoest and Lomov, 2005) (Figure 11).

7.2 Modeling the deformability of the reinforcement and draping

The mechanically based geometrical model of the unit cell (*WiseTex*) can be extended to account for deformation of the fabric (Figure 11b). The aim is first to create a geometry of the deformed unit cell and, second, to calculate resistance

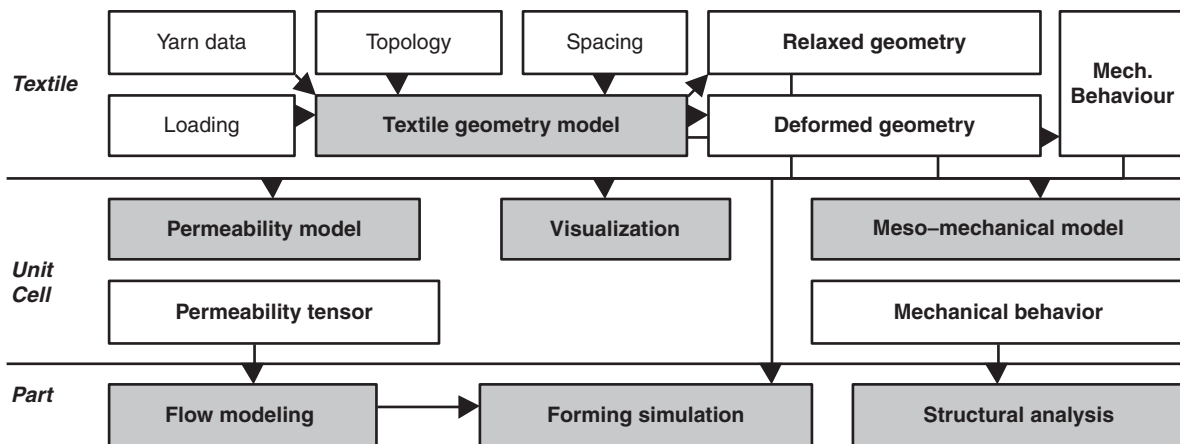


Figure 10. Multi-level structure of modeling tools for textile composites.

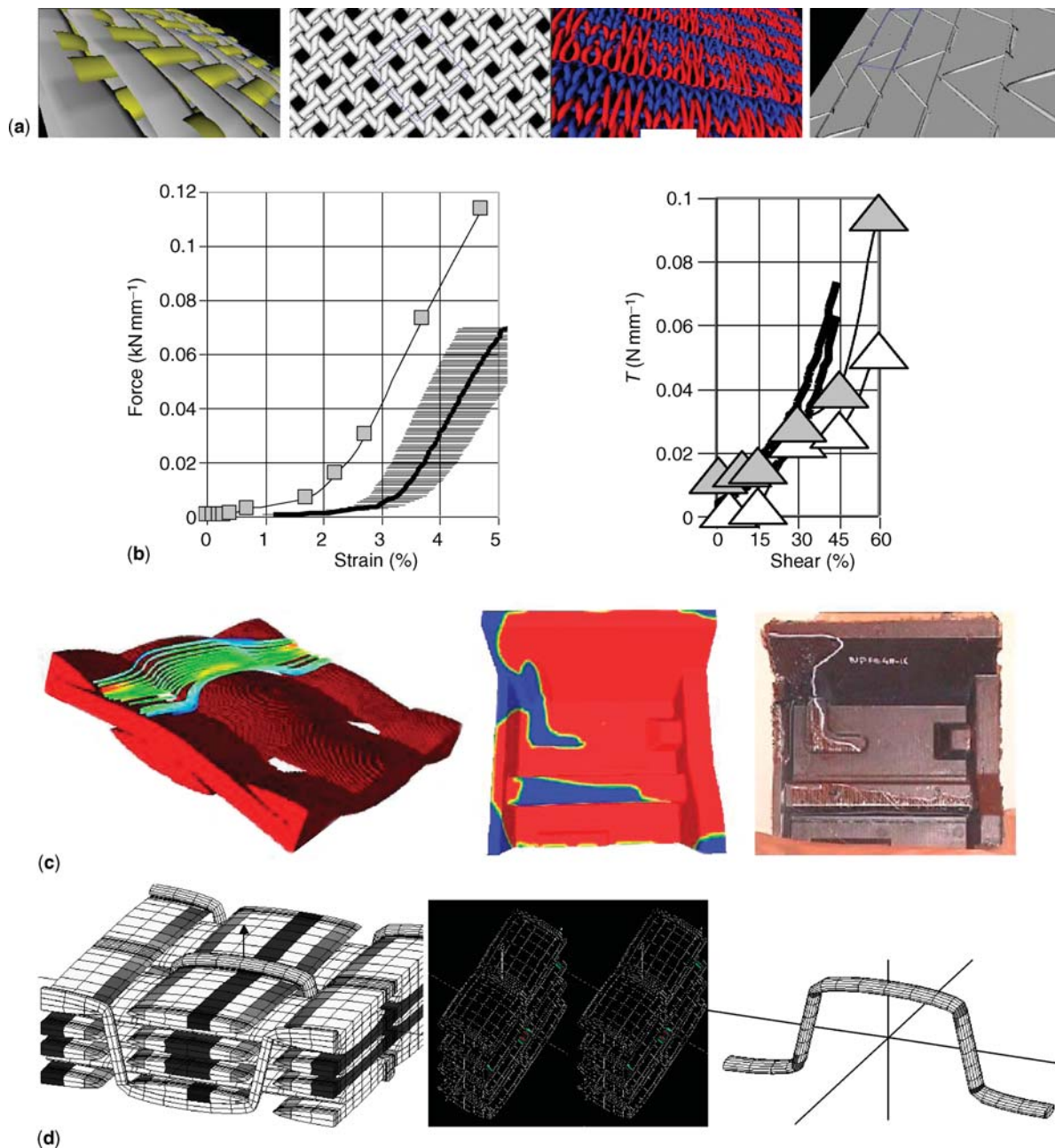


Figure 11. Models of (a) internal structure of woven, braided, knitted, and non-crimp fabrics; (b) tension and shear deformation of the glass woven fabric: full lines denote experiment, points denote calculations; (c) flow through the unit cell and mold-filling simulation; (d) damage pattern in 3D-woven composite (damaged elements shown gray). All simulations based on *WiseTex* unit cell models.

to tension, shear, and compression, that is, predict load-deformation diagrams shown in Figure 4. The models in *WiseTex* are approximate. Using geometrical description and data on compressibility and bending resistance of the yarns, it is possible to simulate more accurately the deformation resistance using finite element model of dry fabric (Boisse *et al.*, 2001, 2008).

The results of the meso-level modeled or experimentally investigated deformability can be used further as input to the draping models, kinematic (not accounting for the shear resistance and placing the directions of two orthogonal yarn systems on the geodesic lines of the mold surface; in this case, only definition of locking angle and other terminal conditions are taken from the meso-modeling or experiment) or finite

element based (in which case full description of behavior is needed). There exist specialized software packages for such a modeling (e.g., PAM-FORM).

7.3 Modeling the permeability and mold filling

With the geometry of the unit cell given, it is quite straightforward to calculate the homogenized permeability tensor of the textile, solving Navier–Stokes or Stokes flow equations for the given pressure gradient (Figure 11c). The difficulties of meshing the complex volume of inter-yarn pores are solved most easily using so-called *voxel* mesh, which consists of brick elements with parallel faces. Each element is labeled as belonging to the pore or to the yarn volume. To account for the permeability of yarns themselves, the Brinkmann equation is used: in this case, the local permeability (calculated using Figure 5a) is assigned to voxels belonging to the yarns. As the geometrical model of the unit cell allows creating the geometry of a sheared/compressed/stretched unit cell, the permeability can be calculated also for the deformed configurations of the textile.

Based on the results of modeling of draping of the reinforcement over the mold and results of the homogenization for deformed unit cells, the local homogenized permeability tensor can be calculated and assigned to the elements of the preform. This information is given to a Darcy solver (see Section 3), for example, PAM-RTM or LIMS, for simulation of the mold filling (Figure 11c).

7.4 Modeling the mechanical properties of textile composites and structural analysis

The geometrical model of the textile unit cell is the starting point for the calculation of the homogenized stiffness of composite. Apart from the orientation averaging (see Section 4), more advanced methods are implemented in the existing software, as the method of inclusions (Mori-Tanaka). Based on the results of modeling of draping of the reinforcement over the mold and on the results of the homogenization for the deformed unit cells, the local homogenized stiffness can be calculated and assigned to the elements of the preform. Structural analysis of the composite part (Figure 10) can then be performed accounting for this variable stiffness (e.g., PAM-SYSPLY software, combined with WiseTex unit cell model and Mori-Tanaka homogenization).

The prediction of strength and progressive damage in textile composite parts (on *macro*-level) is based on failure envelopes and damage models described in the Section 6.3 above. These models are built-in in commercial general-

purpose and specialized FE packages (NASTRAN, ANSYS, ABAQUS, GENOA, PAM-CRASH. . .)

Strength and damage modeling of textile composites can be extended to the level of the unit cell of the reinforcement by *meso*-level FE analysis. An integrated meso-FE modeler should include the following modules:

- *A geometric modeler*, which defines the volumes of yarns and fibrous plies in the unit cell of textile composite and local fiber parameters on the micro-scale, and provides an interface with FE package to export these data;
- *A geometry corrector*, which adapts the geometrical model for requirements of the meshing engine and the particular necessities of boundary condition formulation;
- *A meshing engine*;
- *A material property processor*, which assigns material properties to volumes/elements, using local fiber assembly parameters on micro-scale, provided by the geometrical model, and applying a certain model of homogenization on micro-level, or even a menu for user choice of such a model;
- *Boundary condition routines*, facilitating posing periodic boundary conditions;
- *A FE solver and post-processor*;
- *A homogenization engine*, which automatically applies the necessary loading and boundary conditions, processes the results and outputs the homogenized meso-stiffness matrix of the textile composite;
- *A damage detection processor*, employing one of the (user-chosen) damage initiation criteria;
- *A damage development processor*, responsible for monitoring the damage tensor, change of the homogenized (on micro-level) properties and decisions on the damage propagation modeling.

Figure 11d illustrates a calculation of damage in a 2D woven composite.

8 CONCLUSION

Textile composites offer benefits in the possibilities for automation in cost and in easier applicability of closed-mold processes. The interlaminar, through-the-thickness, impact, and crash properties of textile composites are improved due to interlacing of the yarns in the reinforcements. At the same time, stiffness is downgraded due to the yarn crimp. Well-controlled structures of textiles open possibilities for optimization of fiber placement and production of net-shaped preforms. Development of models and algorithms for prediction of mechanical properties of textile composites and their

behavior during manufacturing brings predictive abilities to the design of textile composite parts.

REFERENCES

- Boisse, P., Buet, K., Gasser, A. and Launay, J. (2001) Meso/macro-mechanical behaviour of textile reinforcements for thin composites. *Compos. Sci. Technol.*, **61**, 395–401.
- Boisse, P., Hamila, N., Helenon, F., Hagege, B. and Cao, J. (2008) Different approaches for woven composite reinforcement forming simulations. *Int. J. Mater. Form.*, **1**, 21–29.
- Chamis, C.C. (1989) Mechanics of composite materials: past, present and future. *J. Compos. Technol. Res.*, **11**(1), 3–14.
- Greve, L. and Pickett, A.K. (2006) Modelling damage and failure in carbon/epoxy non-crimp fabric composites including effects of fabric pre-shear. *Compos. Part A Appl. Sci. Manuf.*, **37**(11), 1983–2001.
- Hinton, E., Kaddour, A.S. and Soden, P.D.(eds) (2004) *Failure Criteria in Fiber Reinforced Polymer Composites: The World-Wide Failure Exercise*, Elsevier, Amsterdam.
- Ladevèze, P. and Le Dantec, E. (1992) Damage modelling of the elementary ply for laminated composites. *Compos. Sci. Technol.*, **43**, 257–267.
- Verpoest, I. and Lomov, S.V. (2005) Virtual textile composites software Wisetex: integration with micro-mechanical, permeability and structural analysis. *Compos. Sci. Technol.*, **65**(15–16), 2563–2574.
- Bogdanovich, A.E. and Pastore, C.M. (1996) *Mechanics of Textile and Laminated Composites*, Chapman and Hall, London.
- Cao, J., Akkerman, R., Boisse, P., Chen, J., Cheng, H.S., Graaf, E.F.d., Gorczyca, J.L., Harrison, P., Hivet, G., Launay, J., Lee, W., Liu, L., Lomov, S.V., Long, A., Luycker, E.d., Morestin, F., Padvoiskis, J., Peng, X.Q., Sherwood, J., Stoilova, T., Tao, X.M., Verpoest, I., Wiggers, J., Willems, A., Yu, T.X. and Zhu, B. (2008) Characterization of mechanical behavior of woven fabrics: experimental methods and benchmark results. *Compos. Part A*, **39**, 1037–1053.
- Chinesta, F. and Cueto, E.(eds) (2007) *Advances in Material Forming. Esaform 10 Years On*, Springer.
- Chou, T.-W. and Ko, F.K. (1989) *Textile Structural Composites*, Elsevier.
- Cox, B. N. and Flanagan, G. (1997) *Handbook of Analytical Methods for Textile Composites*. National Aeronautics and Space Administration, Langley Research Center, Hampton, Virginia.
- Crookston, J.J., Long, A.C. and Jones, I.A. (2005) A summary review of mechanical properties prediction methods for textile reinforced polymer composites. *Proc. Inst. Mech. Eng. Part L.J. Mater. Des. Appl.*, **219**(L2), 91–109.
- Denton, M.J. and Daniels, P.N.(eds) (2002) *Textile Terms and Definitions*, 11th edn, The Textile Institute, Manchester.
- John, S., Herszberg, I. and Coman, F. (2001) Longitudinal and transverse damage taxonomy in woven composite components. *Compos. Part B*, **32**, 659–668.
- Lomov, S.V., Huysmans, G. and Verpoest, I. (2001) Hierarchy of textile structures and architecture of fabric geometric models. *Text. Res. J.*, **71**(6), 534–543.
- Lomov, S.V., Ivanov, D.S., Verpoest, I., Zako, M., Kurashiki, T., Nakai, H. and Hirose, S. (2007) Meso-FE modelling of textile composites: road map, data flow and algorithms. *Compos. Sci. Technol.*, **67**, 1870–1891.
- Lomov, S.V., Ivanov, D.S., Truong Chi, T., Verpoest, I., Baudry, F., Vanden Bosche, K. and Xie, H. (2008) Experimental methodology of study of damage initiation and development in textile composites in uniaxial tensile test. *Compos. Sci. Technol.*, **68**, 2340–2349.
- Long, A.C. (2005) *Design and Manufacture of Textile Composites*, Woodhead Publishing Ltd, Cambridge.

FURTHER READING